The Geological Significance of a Tuffite Interlayer in the Cretaceous Port Island Formation in Northeastern Hong Kong

ZHAO Longlong[1], WANG Lulin[2, *], TIAN Mingzhong[2] and WU Fadong[2]

1 *Key laboratory of Digital Earth Science, Institute of Remote Sensing and Digital Earth, Chinese Academy of Sciences, Beijing 100094, China*

2 *School of Earth Science and Resources, China University of Geosciences, Beijing 100083, China*

Abstract: The Port Island Formation (PIF), a typical Cretaceous red bed in Hong Kong, is dominated by non-fossiliferous, reddish clastic rocks, making it difficult to determine the sedimentary age of PIF precisely. Previous studies assigned the PIF to Late Cretaceous provisionally only on the basis of its stratigraphic sequence and lithology. This study identified a tuffite interlayer in the PIF and a zircon U-Pb age of 128.2±2.7 Ma by LA-ICP-MS method was obtained. It's the first time to date the depositional age of the PIF with a reliable chronological constraint. With the support of stratigraphic evidence, we concluded that the geological age of PIF should be Early Cretaceous rather than Late Cretaceous. Based on the volcanic history of Hong Kong and Southeast China and the distribution of the PIF in Mirs Bay, it is believed that there was no volcanic activity in Hong Kong in ca. 128 Ma. The tuffite interlayer discovered in PIF was formed by the deposition of volcanic ash, which might originate from remote region outside Hong Kong, in an aquatic environment on Port Island. The identification of the tuffite interlayer, as the response to a volcanic event, has great significance not only to the studies of establishment and regional correlation of the strata system and the geological evolution in Hong Kong, but also to the study of volcanic activities in Southeast China.

Key words: tuffite, LA-ICP-MS zircon U-Pb dating, Port Island Formation, Early Cretaceous, volcanic activities, Hong Kong, China

1 Introduction

In the Mesozoic, extensive magmatism occurred along the Southeast China including present-day Hong Kong (Sewell and Campbell, 1997; Sewell et al., 2012a; Li et al., 2014; Zhao Longlong et al., 2017). Under the impact of intensive and destructive volcanism and magmatic intrusion, as well as the regional tectonic movements, sedimentary strata in Hong Kong has a limited distribution and outcrops, and usually are scattered. The strata contact relations are unclear, which create difficulties in establishing the stratigraphic sequence in Hong Kong (Li Zuoming and Lin Jifeng, 1987; Li Xiaochi, 2012).

The Port Island Formation (PIF), named by Ruxton in 1960, is a typical Cretaceous red bed in Hong Kong. It is a continental facies clastic rock formation, dominated by non-fossiliferous, reddish brown conglomerate, sandstone and siltstone deposited in fluvial environment (Jones, 1995; 1996). The PIF crops out on some of the islands in Mirs Bay in northeastern Hong Kong including Port Island, Channel Rock and Round Island and so on. The type section of PIF exposed on the southern coast of the Port Island (Lee, 1985; Lai et al., 1996; Sewell et al., 2000). Boreholes and seismic interpretation show that the PIF is widespread over most of Mirs Bay subcropping the superficial deposits (Lai et al., 1996; Sewell et al., 2000; Zhao Longlong, 2017).

Although many scholars had conducted relevant researches on the formation age of the PIF, it has never been reached an accurate conclusion yet. There are two main reasons: (1) that the PIF formed in an arid saline environment, in which nearly no life can survive, and thus no standard fossils were found in the PIF (Zhang Jiefang, 1987; Li Zuoming and Lin Jifeng, 1987), and (2) that the PIF is mainly composed of clastic rocks and it's hard to find minerals or rocks which can perform isotopic dating.

* Corresponding author. E-mail: 444901281@qq.com

The existing literatures stated that the PIF was thought to be Upper Cretaceous strata according to the lithology and the stratigraphic correlation with neighboring equivalent strata (Lai et al., 1996; Owen, 2000; Sewell et al., 2000; Li Xiaochi, 2012; Tang et al., 2014).

This study for the first time discovered a layer of tuffite in the PIF on the southern coast of Port Island. We examined the tuffite using LA-ICP-MS zircon U-Pb dating method. In combination with the stratigraphic correlation and regional geological data, we confined the depositional age of the PIF, explored the petrogenesis of the tuffite and analyzed the volcanic activities in Hong Kong area of the Cretaceous period. The results have a great significance not only to the studies of establishment and regional correlation of the stratigraphic sequence and the geological evolution in Hong Kong, but also to the study of volcanic activities in Southeast China.

2 Geological Settings

2.1 Regional geology

Southeast China is located at the junction of the Pacific Plate and the Eurasian Plate. It comprises two major crustal blocks: the Yangtze Block in the north and the Cathaysia Block in the south (Fig. 1a), collectively known as the South China Block (Hsü et al., 1990; Jahn et al., 1999; Tang et al., 2014; Ding Cong et al., 2015; Zhao Longlong et al., 2017; Wang Jinrong et al., 2017). During the Late Mesozoic, extensive magmatism occurred in Southeast China, resulted in multi-stage and multi-cycle frequent violent magmatic activies (Wang Dezi and Du Yangsong, 1990; Sewell and Campbell, 1997; Sewell et al., 2012a; Zhou Jian et al., 2012; Zhou Liyun et al., 2016; Jiang Yang et al., 2016; Liu Lei et al., 2017). The Mesozoic igneous rocks formed a 400-km-wide belt along the coastal region of Southeast China (Sewell and Campbell, 1997; Sewell et al., 2012a) (Fig. 1). The igneous rocks are progressively younger from the inland towards the coast (Wang Dezi et al., 2000; Li et al., 2014; Lin Wenjing et al., 2016).

2.2 Hong Kong geology

Hong Kong is located in the southern Cathaysia Block, at the southwestern extremity of the Lianhuashan Fault Zone, which is one of the dominant structural features of Southeast China (Sewell et al., 2000; Wang et al., 2015; Wang Liming et al., 2016) (Fig. 1a). In Guangdong Province, the Lianhuashan Fault Zone is up to 30 km wide and has NNE- and E-trending faults (Bureau of Geology and Mineral Resources of Guangdong Province, 1988). Hong Kong is strictly controlled by the Lianhuashan Fault Zone and the fault structures, trending NEE, NNW and

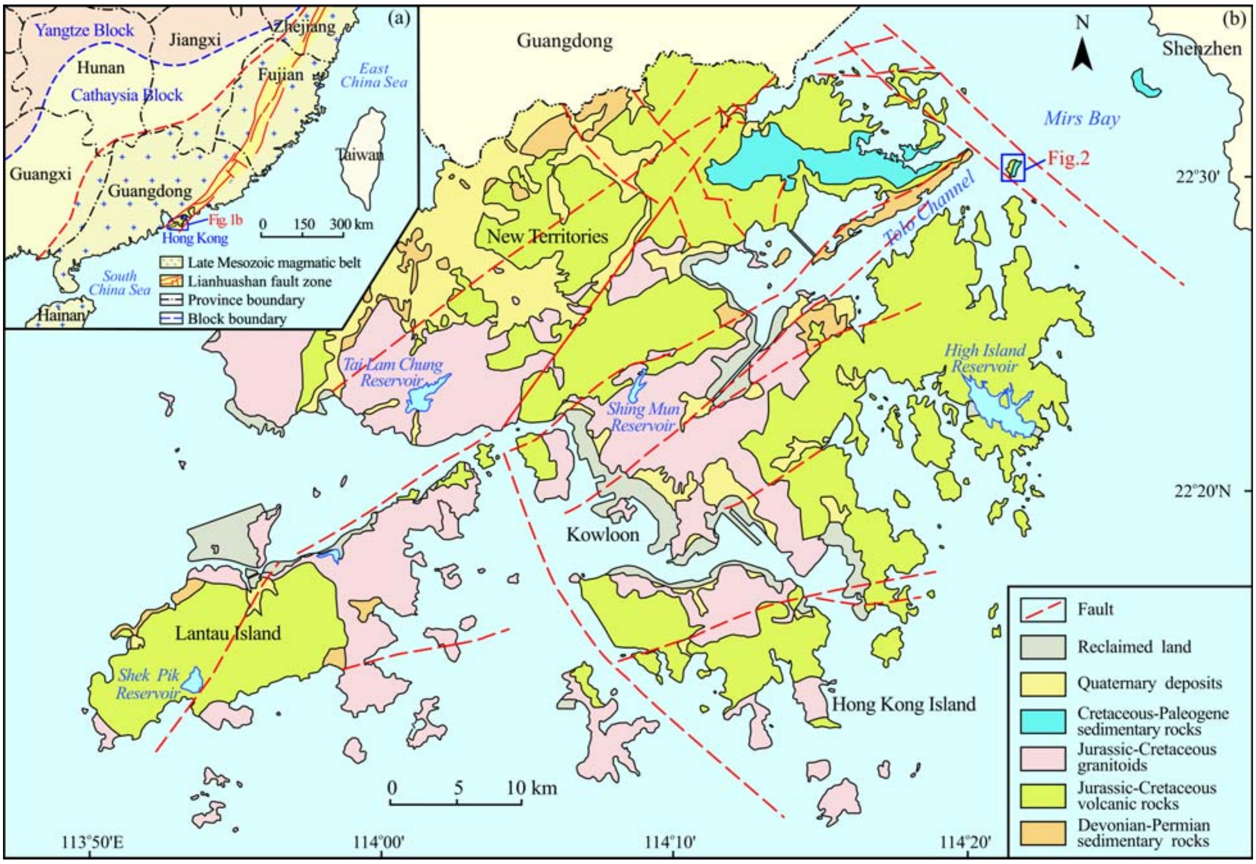

Fig. 1. (a) Regional tectonic map of Southeast China; (b) Simplified geological map of Hong Kong (after Sewell et al., 2000).

NNE, are well developed (Li Zuoming and Lin Jifeng, 1987). The major structural features of northeastern New Territory where the study area is located, are dominated by NE-trending faults, shear zones and fold axes, with subordinate NW- and E-trending faults (Fig. 1b). Identification of folds in the area is difficult as most of them are obscured by intense faulting, magmatism and metamorphism (Lai et al., 1996).

After extensive Mesozoic magmatism, the northeastern New Territories had undergone a relatively stable period, and three fault-depression basins were developed: the Pat Sin Leng Basin, the Tai Pang Wan Basin and the Ap Chau Basin, deposited typical Cretaceous terrigenous red beds which were named the Pat Sin Leng, Port Island and Kat O Formations, collectively known as the Mirs Bay Group (Fig. 1b) (Lai et al., 1996; Li Xiaochi, 2012). All of these formations are dominated by reddish sandstone, siltstone and conglomerate (Lai et al., 1996; Sewell et al., 2000; Tang et al., 2014). The Pat Sin Leng Formation lies unconformably on volcanic rocks of the Tai Mo Shan Formation and shows fault contact relationship with Bluff Head Formation (Geotechnical Engineering Office (GEO), 1992; Lai et al., 1996). The PIF overlies unconformably on volcanic rocks of the Long Harbor Formation and shows conformable contact relationship with its overlying strata the Ping Chau Formation (Lai, 1991; Jones, 1996; Li Zuoming et al., 1997; Li Xiaochi, 2012). The Kat O Formation is likely to be a deposition at the basin edge in similar age as the PIF (Li Zuoming and Lin Jifeng, 1987; Li Xiaochi, 2012). Earlier studies thought the Ping Chau Formation is a Paleogene product, but recent researches put forward that it is very likely to be Cretaceous strata (Wang Lulin et al., 2018).

The stratigraphic section investigated in this paper is located in the southern margin of Port Island in northeastern New Territories. The geological coordinates of starting and ending points are north latitude 22°29'48", east longitude 114°21'30" and north latitude 22°29'49", east longitude 114°21'36" (Fig. 2a). The PIF is unconformably overlying on the Long Harbor Formation, dipping 20–30° to the east-northeast and it can be divided into three members (Figs. 2b and 3a). From the Lower member to the Upper member, rock grain size changes from coarser to finer. A tuffite interlayer of about 2.7 meters thick, was discovered in the Middle member. It is on top of a coarse sandstone layer and under a conglomerate strata with coarse sandstone in it (Figs. 2b and 3b).

3 Sampling and Dating Method

3.1 Sampling and petrographic features

There are two strata on Port Island: the Long Harbor Formation of rhyolitic crystal welded tuff, distributed in the west of the island, and its overlying stratum, the PIF, consists of well bedded and cross-bedded reddish-brown conglomerate, sandstone and siltstone, distributed in the east of the island (Lai et al., 1996; Zhao Longlong et al., 2017) (Fig. 2a). A sample (PS7) was collected from the tuffite interlayer of the PIF on the south margin of the Port Island (Fig. 2). The sample has a massive structure and tuffaceous texture, with a brick-red fresh surface (Fig. 3c). The thin-section photomicrograph of tuffite sample shows that it contains about 65–70% of tuffaceous materials which mainly are vitric fragment and volcanic dust and a small portion of terrigenous clasts. Most of the vitric fragments are out of shape and can faintly see their cambered surface angular shape. They have a littery distribution and have been replaced unevenly by clay and limonite. The terrigenous clasts mainly are lithic fragment, accounts for about 30% of the composition, and quartz. Most of the lithic fragments, 0.1 to 2 mm in size, are distributed promiscuously, subrounded and well sorted. There are a few of gravel-sized grains larger than 2.8 mm. Tuff and siliceous rocks were identified among the lithic fragments which are certain degree of claization and limonitization (Fig. 3d).

3.2 U-Pb dating method

Zircon grain separation was performed in the laboratory of the Regional Geology Minerals Investigation Research Institute, in Hebei Province, China. The coarse sample was washed and crushed. Then zircon grains were separated by standard magnetic and heavy liquid methods and hand-picked under a binocular microscope. Clean, transparent, relatively euhedral zircon crystals without cracks or inclusions were mounted in epoxy blocks, polished to obtain an even surface, and cleaned in an acid bath. The transmitted and reflected light images and cathode luminescence (CL) images of the zircon grains were photographed in Dishi technologies Co. Ltd., Beijing. The analytical positions of zircon grains for isotopic analyses were based on CL images (Fig. 4a), which show the internal texture, morphology and surface cracks of the zircon grains.

The zircon U–Pb isotope analysis was performed at Laser Ablation Inductively Coupled Plasma Mass Spectrometer (LA-ICP-MS) microscopic analysis Laboratory, State Key Laboratory of Geological Processes and Mineral Resources, China University of Geosciences, Beijing. The analytical instruments used were the Thermo Fisher X Series 2 ICP-MS apparatus and the New Wave 193 nm Laser Denudation System. The laser spot beam diameter was 32 μm with a frequency of 8 Hz. For zircon U–Pb dating, NIST610 was used as the external standard to

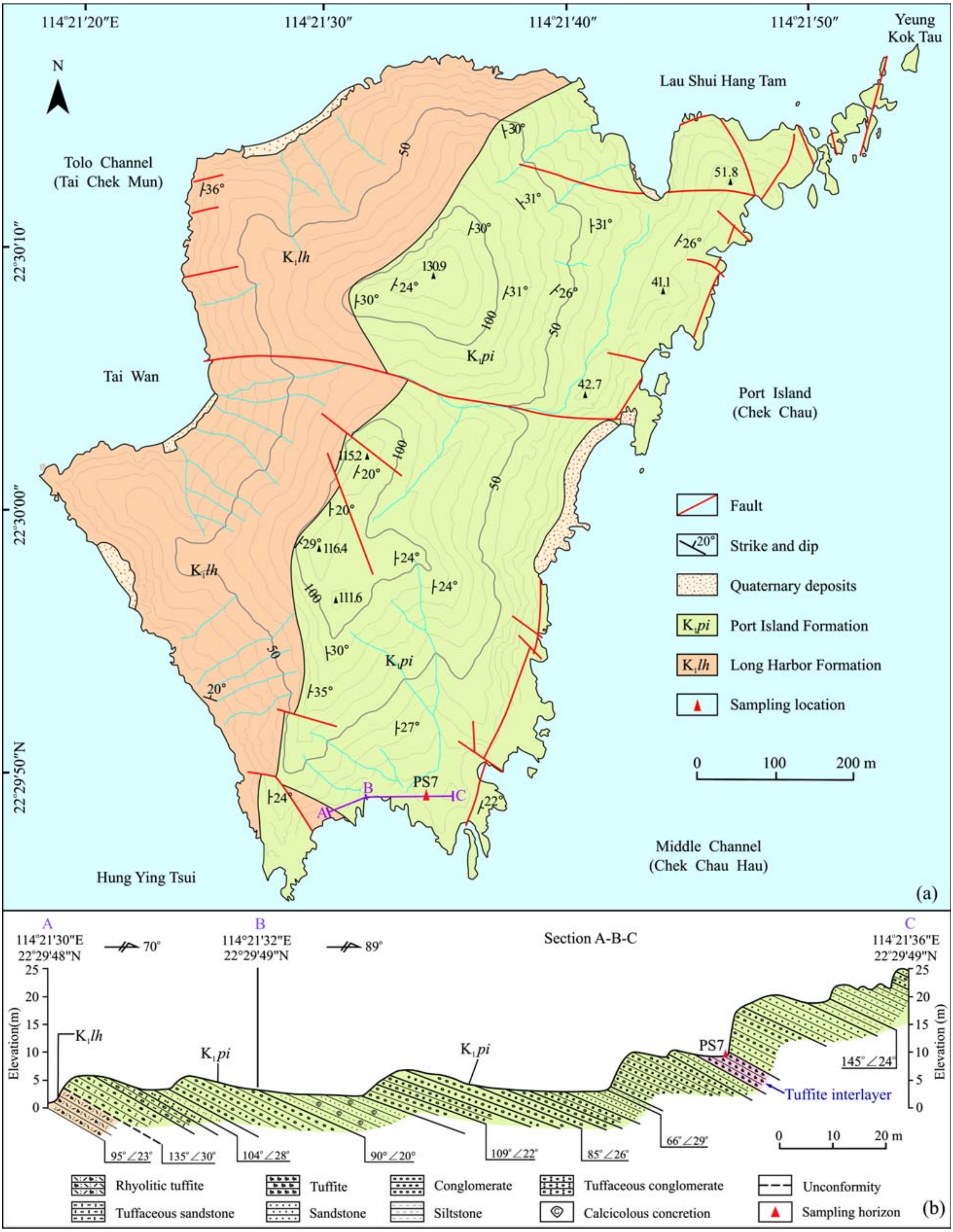

Fig. 2. Simplified geological map of Port Island showing (a) the rocks, strata and sampling location for this study (after Zhao Longlong et al., 2017) and (b) the stratigraphic section of the southern island in which the sampling horizon of tuffite is also shown.

correct the U, Pb, Th contents. Zircon 91500 (Wiedenbeck et al., 1995; 2004) was used as the dating external standard and zircon GJ-1 was used as monitoring standard (Jackson et al., 2004). In the process of isotopic measurement, two

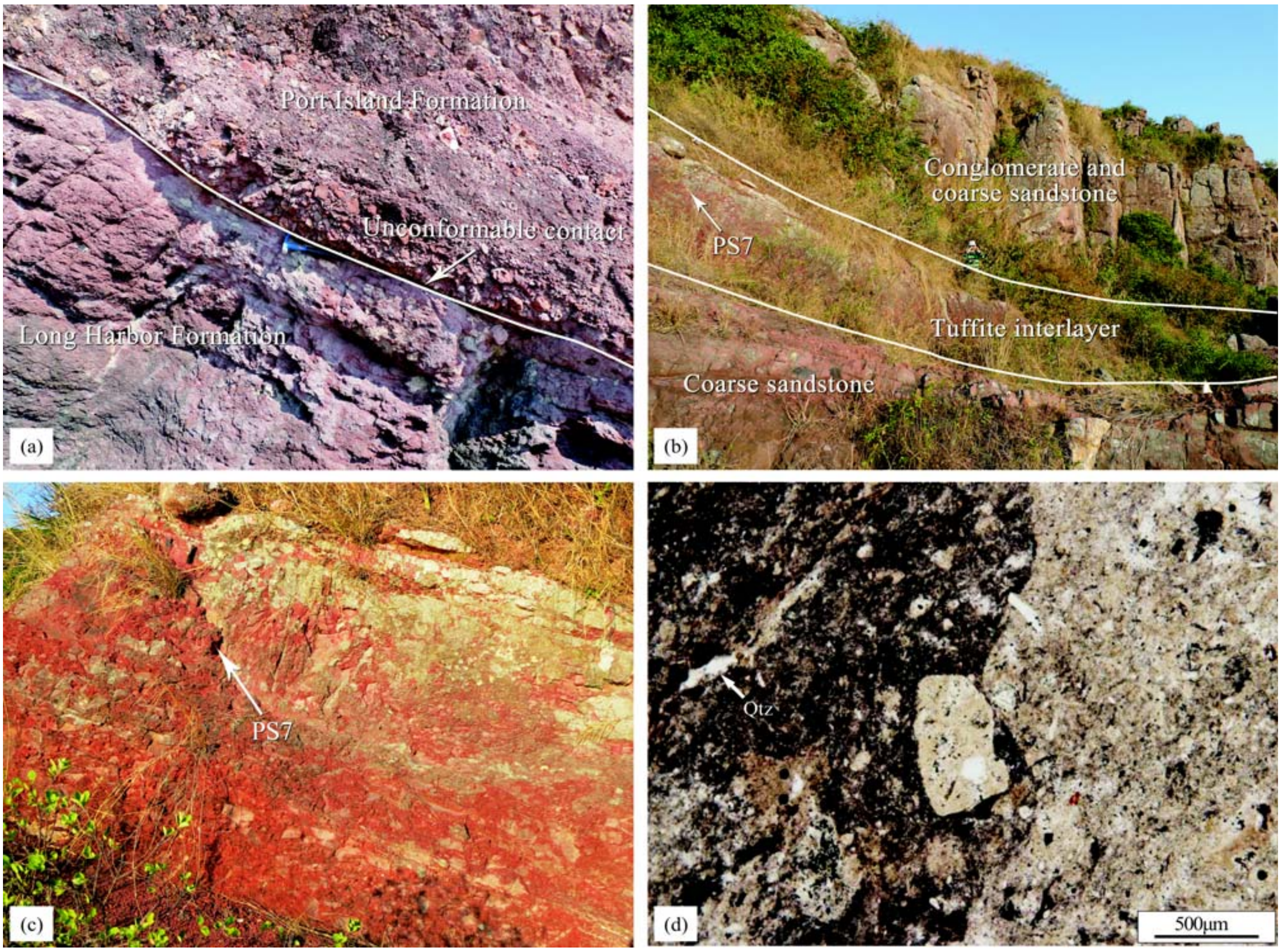

Fig. 3. (a) Unconformable contact of PIF and Long Harbor Formation; (b) Field occurrence of the tuffite interlayer, showing part of middle member of the PIF; (c) Sampling location of sample PS7; (d) Thin-section photomicrographs (plane-polarized light) of sample PS7, Qtz: Quartz.

zircon 91500 samples were repeatedly measured before and after five testing spots, and were analyzed to correct the measurement results of the sample. Analysis was performed only on zircon grains without observable fractures or fluid inclusions. Detailed instrumentation and analytical accuracy description are similar to those described by Liu et al. (2008) and Shen et al. (2012).

The ICPMsDataCal (Liu et al., 2008) program was adopted for ICP-MS data post processing. The zircon age and concordia diagram were obtained using the Isoplot 3.0 (Ludwig, 2003) program. The errors involved in individual spots are all equal to 1s, and the weighted mean $^{206}Pb/^{238}U$ ages have a 95% confidence coefficient. For the details of the zircon U-Pb isotopic age analytical method, procedures and analytical accuracy description, refer to Gao et al. (2002) and Wang et al. (2012a, b).

4 U-Pb Dating Result

4.1 Zircon characteristics

Zircon grains are relatively abundant in tuffite sample PS7. The zircon grains are euhedral or subhedral. Most of them are long prismatic, and a small number of them are short prismatic. They generally range up to 100–200 μm in length and 60–120 μm in width. The length/width ratios range from 1 to 2.5. In CL images, the interior of the zircons shows planar growth and typical magmatogenic oscillatory zoning (Fig. 4a).

Twenty-three spot analyses were performed on the zircon grains of PS7 and all of the positions were marked on the CL images (Fig. 4a). The in situ analyses of rare earth elements (REEs) contents of zircon grains in tuffite sample are shown in Table 1. All zircon grains have high ΣREE contents, ranging from 791.38 to 2325.15 ppm, with an average of 1386.05 ppm. In the chondrite normalized REE distributions patterns (Boynton, 1984) (Fig. 5), all the zircon grains show depletion of light rare earth elements (LREEs), strong enrichment of heavy rare earth elements (HREEs), obvious positive Ce anomalies (δCe=4.27–323.52, average 37.10) and negative Eu anomalies (δEu=0.05–0.38, average 0.19) (Fig. 4a). All these characteristics are in accordance with the features of

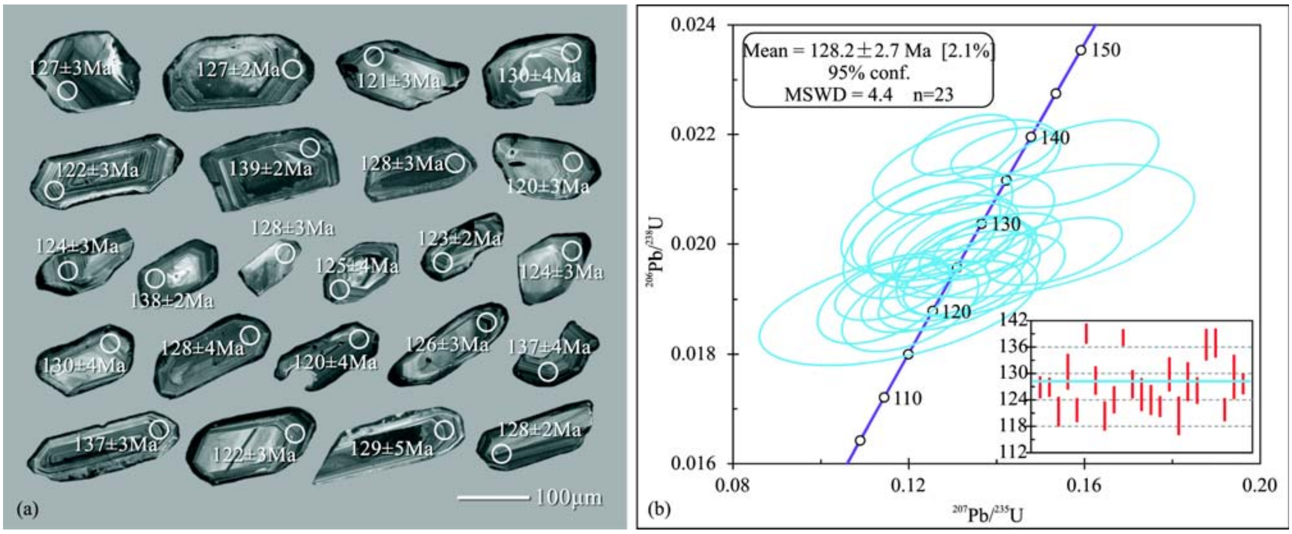

Fig. 4. (a) CL image, testing spot locations and spot ages of PS7; (b) U-Pb concordia diagram of PS7.

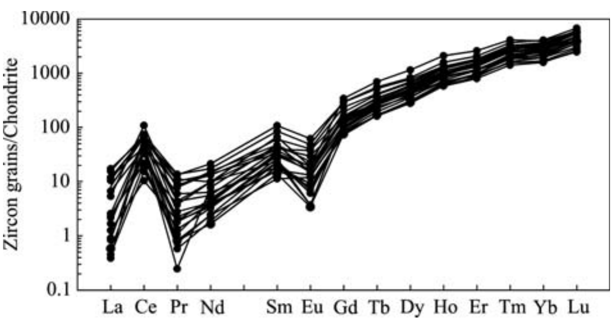

Fig. 5. Chondrite normalized REE patterns (after Boynton, 1984) of zircon grains in tuffite of the PIF.

a typical magmatic zircon (Buick et al., 1995; Belousova et al., 2002; Xie Qifeng et al., 2017). A large number of studies show that magmatic zircons are rich in Th and U contents and the Th/U ratios are normally higher than 0.4 (Hidaka et al., 2002; Wu Yuanbao and Zheng Yongfei, 2004). In this study, U content of the zircons is 215.54–931.55 ppm and the Th content is 238.98–2114.43 ppm, Th/U ratio is 0.30–1.32, with an average of 0.69 (only two Th/U ratios are lower than 0.4), the above figures are also consistent with the characteristics of magmatic origin zircons (Liu et al., 2013; Yuan Qian et al., 2014).

Given the above, we concluded that the zircons selected from the tuffite sample are magmatogenic, thus the dated age of these zircons is representative for the formation age of the tuffite interlayer.

4.2 Zircon U-Pb age of the tuffite

The corrected LA-ICP-MS zircon U-Pb data of twenty-three test spots are listed in Table 2. The data from the spot analysis were spread along the concordia line (Fig. 4b). All data fall within a narrow range (^{206}Pb/^{238}U ages: 139±2 Ma to 120±3 Ma) and yield a weighted mean ^{206}Pb/^{238}U age of 128.2±2.7 Ma (95% confidence, MSWD=4.4) (Fig. 4; Table 2). Combining the dated age with the features of zircons, we thought the tuffite interlayer, recorded an obvious volcanic activity during the deposition of PIF, were formed in 128.2±2.7 Ma, and this U-Pb age, to a certain extent, constrains the sedimentary time of the PIF.

5 Discussion

5.1 Formation age of the PIF

It's very difficult to date the accurate age of the PIF because the outcrop of PIF in Hong Kong is limited and the contact relation of the strata is obscured and no fossils have been found in the formation yet. In the past few decades, a number of scholars had studied the formation age of the PIF. Williams (1943) and Davis (1953) thought that the PIF was formed in the Eocene. Allen and Stephens (1971) strongly recommended that the PIF was deposited in Early Cretaceous. However, none of these hypothesizes were supported by fossil evidence. Zhang Jiefang (1987) reported that there were stonewort fossils of *Atopochara* sp. immature individual in PIF and assigned PIF into the age of late Early Cretaceous to early Late Cretaceous according to the morphological characteristics and preservation condition of the fossils. Whereas, the stonewort fossils have not been verified when Li Zuoming et al. (1997) identified them for a second time. They took more than 100 samples from PIF, but none of them contained a fossil. By comparing the PIF to the Nanxiong Group or the equivalent strata in Guangdong Province, Li Zuoming et al. (1997) designated PIF a Late Cretaceous formation provisionally. Some other scholars compared the PIF to the fossil-bearing Lower to Upper Cretaceous

Table 1 Rare earth elements (ppm) contents of zircon grains in tuffite sample from PIF

Test spot No.	La	Ce	Pr	Nd	Sm	Eu	Gd	Tb	Dy	Ho	Er	Tm	Yb	Lu	ΣREE	ΣHREE	δEu	δCe
PS7-1	0.18	17.09	0.10	0.99	2.70	0.25	19.55	8.08	93.17	44.33	204.43	64.43	511.68	128.77	1095.75	1074.44	0.08	30.21
PS7-2	2.50	53.76	0.97	9.22	9.27	1.70	49.24	18.88	211.55	91.53	370.06	105.27	753.94	187.63	1865.52	1788.10	0.19	8.31
PS7-3	0.80	47.79	0.53	3.36	7.31	1.37	41.74	15.77	194.50	86.95	357.34	103.44	734.09	192.32	1787.31	1726.15	0.19	17.08
PS7-4	<0.01	14.47	0.09	1.47	4.42	0.45	25.16	11.18	118.42	50.03	194.98	50.80	338.47	81.64	891.58	870.68	0.10	48.55
PS7-5	2.06	33.61	0.73	3.80	3.60	0.68	20.48	7.95	99.31	47.75	204.59	59.10	466.65	126.02	1076.33	1031.85	0.19	6.59
PS7-6	0.28	27.62	0.27	2.39	3.19	0.97	22.25	9.12	113.00	53.33	233.70	71.88	535.71	151.94	1225.65	1190.93	0.26	21.94
PS7-7	0.14	12.42	0.16	1.93	5.15	0.27	35.00	14.61	181.19	78.92	316.41	83.74	555.78	136.39	1422.11	1402.04	0.05	17.44
PS7-8	3.67	54.04	1.36	5.93	4.58	0.51	24.14	10.32	129.78	59.25	245.08	68.60	501.40	131.51	1240.17	1170.08	0.12	5.82
PS7-9	1.66	87.46	0.53	5.93	7.72	2.77	41.41	13.17	132.43	50.84	188.45	50.58	351.40	93.35	1027.70	921.63	0.38	22.32
PS7-10	0.52	47.19	1.62	12.75	20.99	4.55	74.78	24.35	247.18	96.78	365.61	93.24	621.56	154.45	1765.57	1677.95	0.31	7.81
PS7-11	0.26	36.22	0.13	2.63	5.76	1.18	37.98	13.73	165.78	77.45	327.25	91.69	665.02	183.08	1608.16	1561.98	0.18	47.08
PS7-12	4.83	59.89	1.66	10.45	16.55	3.55	76.35	26.10	265.08	113.32	433.13	118.39	848.60	224.04	2201.94	2105.01	0.25	5.08
PS7-13	3.67	35.52	1.07	7.88	8.07	2.16	32.62	13.56	143.23	62.45	244.56	64.04	440.06	114.97	1173.86	1115.49	0.35	4.27
PS7-14	0.73	17.60	0.46	5.89	13.02	1.39	88.58	32.81	367.63	150.27	543.41	132.26	814.16	196.03	2364.24	2325.15	0.09	7.11
PS7-15	<0.01	32.14	0.03	4.67	9.16	1.12	37.74	13.55	154.94	69.14	275.72	78.44	561.03	151.54	1389.22	1342.10	0.16	323.52
PS7-16	3.23	58.94	0.95	8.65	11.81	2.93	60.76	19.65	223.48	95.75	382.06	104.98	734.95	204.20	1912.34	1825.83	0.27	8.01
PS7-17	0.67	27.16	0.22	2.24	3.08	0.69	18.84	7.84	93.17	42.17	180.71	53.00	403.85	117.16	950.80	916.74	0.21	16.96
PS7-18	0.28	26.11	0.07	1.12	3.81	0.57	22.11	7.67	89.64	41.74	167.47	45.71	331.75	85.29	823.34	791.38	0.15	43.76
PS7-19	5.33	53.23	1.24	8.27	6.40	1.40	35.32	12.72	147.65	69.46	302.69	88.24	672.53	184.18	1588.66	1512.79	0.23	4.82
PS7-20	0.39	8.40	0.23	2.04	4.43	0.27	31.69	12.15	140.13	60.76	235.34	60.02	400.82	100.70	1057.37	1041.61	0.05	6.61
PS7-21	<0.01	31.88	0.10	1.44	2.20	0.88	26.35	12.19	140.04	64.75	291.32	81.75	618.80	177.17	1448.87	1412.37	0.21	96.27
PS7-22	0.12	58.44	0.34	2.44	6.64	1.09	29.52	12.89	158.85	72.42	301.76	83.49	583.99	160.63	1472.62	1403.55	0.20	45.57
PS7-23	<0.01	44.31	0.23	2.88	6.16	1.14	41.86	16.50	186.05	86.38	355.83	95.45	696.36	192.77	1725.92	1671.20	0.16	58.18

Table 2 LA-ICP-MS zircon U-Pb data of tuffite sample from PIF

Test spot No.	Isotopic content (ppm)			Isotopic ratio							Age (Ma)					
	Pb	Th	U	Th/U	$^{207}Pb/^{206}Pb$	1σ	$^{207}Pb/^{235}U$	1σ	$^{206}Pb/^{238}U$	1σ	$^{207}Pb/^{206}Pb$	1σ	$^{207}Pb/^{235}U$	1σ	$^{206}Pb/^{238}U$	1σ
PS7-1	56.85	931.55	1759.91	0.53	0.0557	0.0039	0.1530	0.0103	0.0199	0.0004	443	156	145	9	127	3
PS7-2	41.89	534.00	1442.85	0.37	0.0489	0.0032	0.1357	0.0088	0.0199	0.0003	146	154	129	8	127	2
PS7-3	15.06	255.85	518.28	0.49	0.0443	0.0049	0.1146	0.0101	0.0190	0.0005	87	348	110	9	121	3
PS7-4	15.50	300.28	437.75	0.69	0.0445	0.0053	0.1242	0.0129	0.0204	0.0006	35	293	119	12	130	4
PS7-5	15.94	433.33	465.63	0.93	0.0476	0.0044	0.1238	0.0096	0.0191	0.0004	80	207	119	9	122	3
PS7-6	41.69	411.86	1376.50	0.30	0.0445	0.0029	0.1327	0.0079	0.0218	0.0004	32	137	127	7	139	2
PS7-7	17.76	391.12	532.95	0.73	0.0465	0.0045	0.1278	0.0113	0.0201	0.0005	33	209	122	10	128	3
PS7-8	12.85	228.32	449.76	0.51	0.0494	0.0054	0.1204	0.0103	0.0188	0.0005	165	302	115	9	120	3
PS7-9	14.93	276.95	521.74	0.53	0.0513	0.0052	0.1372	0.0121	0.0194	0.0005	254	39	131	11	124	3
PS7-10	63.38	779.72	2114.43	0.37	0.0470	0.0027	0.1415	0.0079	0.0217	0.0003	50	133	134	7	138	2
PS7-11	11.45	224.48	368.17	0.61	0.0461	0.0048	0.1280	0.0113	0.0200	0.0005	400	−165	122	10	128	3
PS7-12	24.56	467.91	835.73	0.56	0.0497	0.0042	0.1327	0.0102	0.0196	0.0006	189	180	127	9	125	4
PS7-13	12.37	310.61	395.96	0.78	0.0501	0.0054	0.1318	0.0120	0.0194	0.0005	198	230	126	11	124	3
PS7-14	17.27	357.77	572.68	0.62	0.0447	0.0038	0.1162	0.0086	0.0192	0.0004	13	200	112	8	123	2
PS7-15	8.41	215.54	238.98	0.90	0.0491	0.0068	0.1301	0.0152	0.0203	0.0006	150	306	124	14	130	4
PS7-16	13.85	383.56	468.97	0.82	0.0454	0.0078	0.1177	0.0209	0.0188	0.0007	48	256	113	19	120	4
PS7-17	11.41	330.76	348.24	0.95	0.0468	0.0056	0.1230	0.0118	0.0201	0.0007	35	267	118	11	128	4
PS7-18	24.90	921.38	700.60	1.32	0.0493	0.0040	0.1321	0.0100	0.0198	0.0005	165	178	126	9	126	3
PS7-19	13.22	264.93	443.77	0.60	0.0471	0.0060	0.1332	0.0141	0.0214	0.0006	54	291	127	13	137	4
PS7-20	20.22	285.66	637.79	0.45	0.0531	0.0043	0.1579	0.0125	0.0215	0.0005	332	153	149	11	137	3
PS7-21	21.42	558.22	663.98	0.84	0.0487	0.0041	0.1295	0.0108	0.0191	0.0004	200	124	124	10	122	3
PS7-22	10.73	301.17	284.89	1.06	0.0520	0.0091	0.1506	0.0227	0.0202	0.0008	287	356	142	20	129	5
PS7-23	23.21	638.71	708.45	0.90	0.0506	0.0038	0.1402	0.0096	0.0200	0.0004	233	174	133	9	128	2

Baihedong, Sanshui and the Dalangshan Formations in eastern Guangdong Province, and thought that the PIF should be Upper Cretaceous (Lai et al., 1996; Owen, 2000; Sewell et al., 2000; Li Xiaochi, 2012; Tang et al., 2014). In a word, the stratigraphic age of the PIF in current studies is constrained by the lithology and the stratigraphic correlation with neighboring equivalent strata.

Field investigation of this study showed that the 2.7m tuffite interlayer extends steadily along the strike. The zircon grains in the tuffite sample are euhedral or subhedral and hardly have been rounded, which means that the tuffite was almost a direct deposition of volcanic ash fall and there was little or no transportation involved. Therefore, the dated age of the tuffite can be used to constrain the formation time of the PIF. A zircon U-Pb age of 128.2±2.7 Ma of the tuffite was obtained by LA-ICP-MS method, it is the first time a precise and reliable chronological evidence of PIF was obtained. As mentioned above, the tuffite interlayer is situated in the Middle member of the PIF, we speculated that the PIF was still under the deposition process in middle Early Cretaceous according to the stratigraphic chart of China (Yao Jianxin et al., 2016). Recently, several scholars studied the unique rock layer, 0.8m in thickness, of the Ping Chau Formation which is the overlying stratum of the PIF, and found that the lithology of the rock layer was rhyolitic tuff instead of flint or silicalite. They obtained an age of Early Cretaceous for the rock layer and thought the Ping Chau Formation was formed in Early Cretaceous other than Paleogene (Wang Lulin et al., 2018). Though whether the contact relationship between Ping Chau Formation and the PIF is conformity or not remains controversial (Lai et al., 1996; Li Zuoming et al., 1997; Li Xiaochi, 2012), the depositional age of Ping Chau Formation is later than that of the PIF is widely accepted, thus we suggested that the PIF deposition ended in Early Cretaceous. Furthermore, it is universally acknowledged that the Long Harbor Formation, underlying stratum of the PIF, was formed in Early Cretaceous (Davis et al., 1997; Sewell et al., 2000; Campbell et al., 2007; Sewell et al., 2012a, b; Zhao Longlong et al., 2017).

To sum up, based on the age of the tuffite found in the PIF and the stratigraphic sequence relation, we proposed that the depositional age of the PIF is Early Cretaceous instead of the Late Cretaceous. Thus, much of the knowledge of the stratigraphic sequence and geological evolution in Hong Kong require further study and revision.

5.2 Volcanic activities in Southeastern China

Previous studies divided the Mesozoic magmatism of Hong Kong into four main episodes, from the Middle Jurassic (J_2) to the Early Cretaceous (K_1): 164–160 Ma, 148–146 Ma, 144–142 Ma and 141–140 Ma (Campbell and Sewell, 1997; Davis et al., 1997; Sewell et al., 2000, 2012a, b; Campbell et al., 2007; Li et al., 2014) (Table 3). Corresponding to the four magmatic episodes are four volcanic groups and coeval granitoid suites (Sewell et al., 2012a, b; Tang et al., 2014; Zhao Longlong et al., 2017) (Table 3). In general, igneous rocks of the four episodes have a zonal distribution of older ones at the northwest and younger ones at the southeast. This pattern is consistent with the other igneous rocks of the same period along the coast of Southeast China (Wang Dezi et al., 2000; Li et al., 2012; Li et al., 2014； Zhao Longlong et al., 2017).

Regional outcrop feature of the tuffite, product of pyroclastic deposition, is the direct evidence of the intermittent volcanic eruptions (Chen Shuwang et al., 2001). The discovery of the tuffite interlayer in PIF and its isotopic dating provide new information for the study of volcanic activities in Hong Kong as well as in Southeast China.

There are two explanations for the petrogenesis of the tuffite interlayer in this study: (1) that in ca. 128 Ma, there has been a small-scale volcanic eruption in Hong Kong, and according to the younging trend from inland to coastal of magmatism in Hong Kong and in Southeast China, we presumed that the volcanic eruption most likely occurred in Mirs Bay, or (2) that there was no volcanic activity in Hong Kong at that time, and the volcanic ash of the tuffite in PIF originated from the remote region outside Hong Kong such as the eastern Guangdong or Mirs Peninsula in Shenzhen. Volcanic ash of volcanic eruption floated and fell to the Port Island which was an aquatic environment at that time and formed the tuffite layer.

Boreholes and seismic data show that the PIF is widespread over most of Mirs Bay and extends eastward to Xiasha in Shenzhen on the east of Mirs Bay, forming a gentle synclinal basin of 24 km long and 13 km wide with a maximum thickness of 1200 m (Lai et al., 1996) (Fig. 6). In addition, so far, there are no reports on the occurrence of volcanic activity later than 140 Ma in the mainland of Hong Kong. Thus it can be considered that the volcanic activity was unlikely to occur in the Mirs Bay area during the deposition of the PIF. Li Zhaonai et al. (2003) proposed that the Late Jurassic to Early Cretaceous was the heyday of Mesozoic magmatism in Southeast China during 155–125 Ma, and the magmatism at the south margin of eastern Guangdong started earlier and lasted longer than eastern Fujian and Zhejiang. The U-Pb age obtained in this study is exactly fall within this period. The Mesozoic volcanic strata distribution area in Shenzhen is an important part of the volcanic belt in Southeast China, and the Mirs Peninsula, across the Mirs Bay from Port

Table 3 Summary of Middle Jurassic to Early Cretaceous volcanic-plutonic associations in Hong Kong[a]

Magmatic episode	Volcanic group		Granitic suite		Age[b] (Ma)
	Name	Main distribution	Name	Main distribution	
1	Tsuen Wan Volcanic Group (TWVG)	NE and NW New Territories	Lamma Suite (LS): A-type Subsuite, I-type Subsuite	Central and W New Territories, Lamma and Lantau	164–160
2	Lantau Volcanic Group (LVG)	Central and W Lantau	Kwai Chung Suite (KCS)	E Lantau and S New Territories	148–146
3	Repulse Bay Volcanic Group (RBVG): Rhyolitic Subgroup (R), Trachytic Subgroup (T)	S Hong Kong, N Kowloon and Sai Kung	Cheung Chau Suite (CCS)	W Lantau and S New Territories	144–142
4	Kau Sai Chau Volcanic Group (KSCVG)	E New Territories	Lion Rock Suite (LRS): Granite Subsuite (G), Quartz Monzonite Subsuite (M)	N Hong Kong, Kowloon and E Lamma	141–140

Note: a. After Sewell et al. (2012b); b. Based on high precision U-Pb ages (after Davis et al., 1997; Campbell et al., 2007; Sewell et al., 2012a, b; Zhao Longlong et al., 2017).

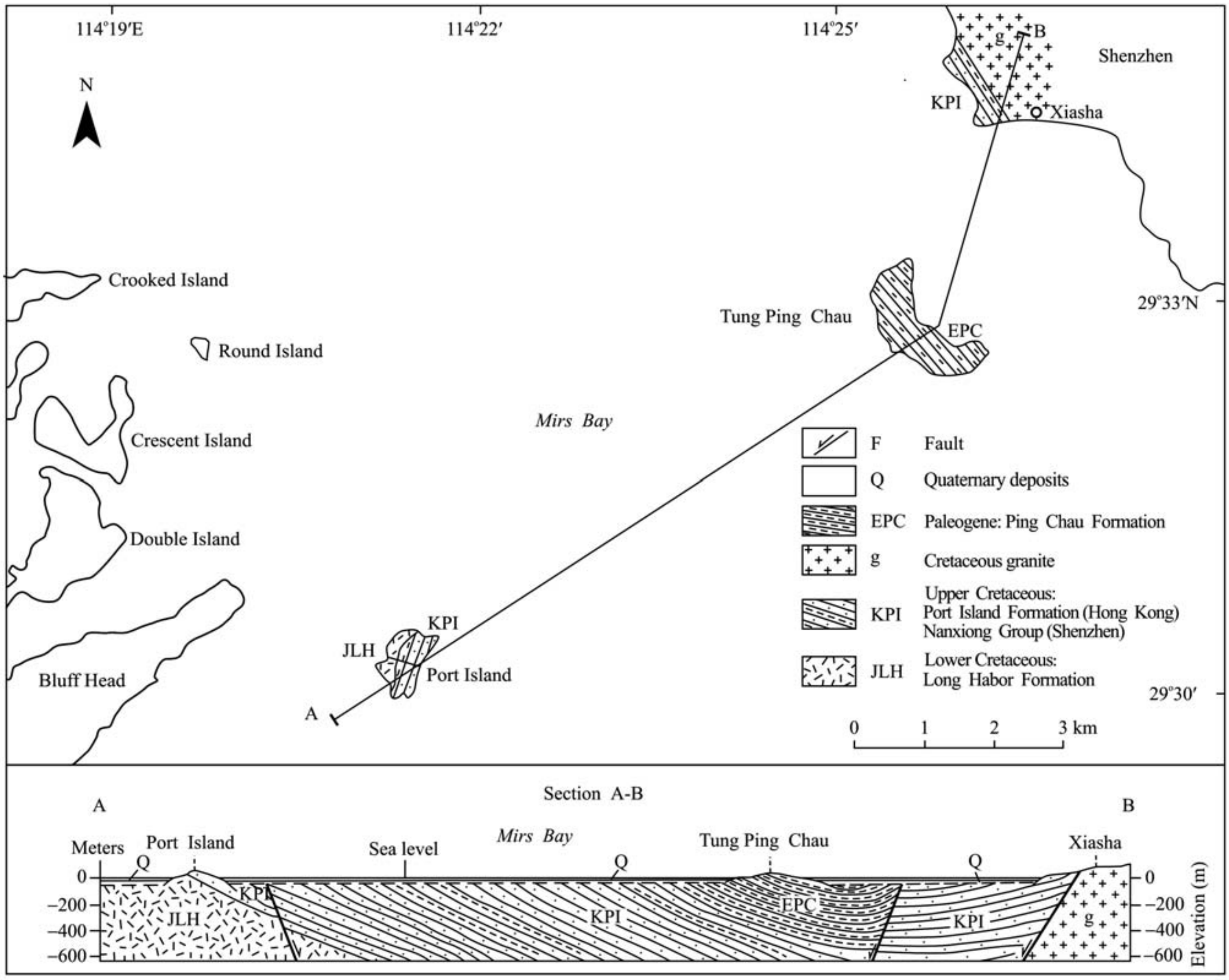

Fig. 6. Geological cross-section of the Sedimentary basin in Mirs Bay (after Lai et al., 1996).

Island, is a representative section of the Jurassic-Cretaceous volcanic strata in Southeast China (Mei Cun et al., 2011). Volcanic ash produced by the volcanic eruptions in Shenzhen may provide abundant materials for the formation of the tuffite interlayer of the PIF.

In the meantime, according to the morphological characteristics of the zircon grains picked from the tuffite sample, enhedral or subhedral and hardly have been rounded, we speculated that the tuffite is original and it was a direct deposition of volcanic ash fall.

Given the above, we estimated that no volcanic activities occurred in Hong Kong during the period of ca. 128 Ma. The tuffite interlayer discovered in PIF was formed by the deposition of volcanic ash, which was produced by volcanic eruption in remote region outside Hong Kong, transported by wind, and fell into the aquatic environment of Port Island. As an important record of a geological event, the tuffite interlayer revealed a volcanic activity in Early Cretaceous and provided new information for the research on the chronology of volcanic activity in Southeast China.

6 Conclusions

This study has a breakthrough discovery of a tuffite interlayer of the PIF in northeastern Hong Kong. After conducting zircon U-Pb dating to a tuffite sample, we reached the following conclusion:

(1) Zircon U-Pb dating of the tuffite interlayer of the PIF yielded an age of 128.2±2.7 Ma. Combined the dated age with the stratigraphic sequence analysis, we concluded that the PIF was formed in Early Cretaceous. It is the first time the depositional age of PIF has been accurately dated. This progress has a great significance to the studies of establishment and regional correlation of the stratigraphic sequence and the geological evolution of Hong Kong.

(2) Based on previous studies on volcanic activities in Hong Kong and Southeast China and distribution of the PIF in Mirs Bay, we deduced that there was no volcanic activity in Hong Kong in ca. 128 Ma. However, the

regional outcrop of the tuffite interlayer is new evidence and provided hints for the research of volcanism chronology in Southeast China in Early Cretaceous.

(3) According to the distribution of the PIF in Mirs Bay and the Cretaceous volcanic activities in Southeast China, we put forward that the tuffite interlayer discovered in PIF was formed by the deposition of volcanic ash in an aquatic environment on the Port Island. The volcanic ash might originate from volcanic eruption in remote region outside Hong Kong, such as the eastern Guangdong or Mirs Peninsula.

Acknowledgements

This study was supported by the Youth Innovation Promotion Association CAS (2017085) and geological survey program of Agriculture, Fisheries and Conservation Department of Hong Kong Special Administrative Region (AFCD/SQ/92/14). We are very grateful to Profs. Cheng Jie and Zhang Xujiao for their guidance in field investigation. We are very grateful to Dr. Ka-ming Yeung, Alvin Ng and T. K. Woo of the AFCD for their help during the field investigation. The constructive comments of the anonymous reviewers are greatly appreciated.

Manuscript received Nov. 1. 2017
accepted Jan. 22, 2018
edited by Fei Hongcai

References

Allen, P.M., and Stephens, E.A., 1971. *Report on the Geological Survey of Hong Kong (1967–1969)*. Hong Kong: Hong Kong Government Printer, 107.

Belousova, E.A., Griffin, W.L., and O'Reilly, S.Y., 2002. Igneous zircon: Trace element composition as an indicator of source rock type. *Contributions to Mineralogy and Petrology*, 143: 602–622.

Boynton, W.V., 1984. Geochemistry of the rare earth elements: meteorite Studies. In: Henserson, P. (ed.), *Rare Earth Element Geochemistry*. Geochemistry, 2: 63–114.

Buick, R., Thornett, J.R., and McNaughton, N.J., 1995. Record of emergent continental crust similar to 3.5 billion years ago in the Pilbara craton of Australia. *Nature*, 375: 574–575.

Bureau of Geology and Mineral Resources of Guangdong Province (BGMRGP), 1988. *Regional Geology of Guangdong Province*. Beijing: Geological Publishing House, 941 (in Chinese).

Campbell, S.D.G., and Sewell, R.J., 1997. Structural control and tectonic setting of Mesozoic volcanism in Hong Kong. *Journal of the Geological Society*, 154: 1039–1052.

Campbell, S.D.G., Sewell, R.J., Davis, D.W., and So, A.C.T., 2007. New U-Pb age and geochemical constraints on the stratigraphy and distribution of the Lantau Volcanic Group, Hong Kong. *Journal of Asian Earth Sciences*, 31: 139–152.

Chen Shuwang, Zhang Lidong, Guo Shengzhe, Zhang Changjie, Peng Yandong, Jia Bin, Xing Dehe, Ding Qiuhong and Zheng Yuejuan, 2001. Discovery of sedimentary tuff beds in basic and intermediate-basic volcanic rocks of Yixia Formation in west Liaoning Province and its significance. *Liaoning Geology*, 18(1): 52–57 (in Chinese with English abstract).

Davis, D.W., 1953. *The Geology of Hong Kong*. Hong Kong: Hong Kong Government Printer, 210.

Davis, D.W., Sewell, R.J., and Campbell, S.D.G., 1997. U-Pb dating of Mesozoic igneous rocks from Hong Kong. *Journal of the Geological Society*, 154 (6): 1067–1076.

Ding Cong, Zhao Zhidan, Yang Jinbao, Zhou Hongfang, Sheng Dan, Hou Qingye and Hu Zhaochu, 2015. Geochronology, geochemistry of the Cretaceous granitoids and mafic to intermediate dykes in Shishi area, coastal Fujian Province, *Acta Petrologica Sinica*, 31(5): 1433–1447 (in Chinese with English abstract).

Gao, S., Liu, X.M., Yuan, H.L., Harttendorf, B., Gunther, D., and Hu, S.H., 2002. Determination of forty-two major and trace elements of USGS and NISTSRM glasses by laser ablation inductively-coupled plasma mass spectrometry. *Geostandards and Geoanalytical Research*, 26 (2): 181–196.

Geotechnical Engineering Office (GEO), 1992. Kat O Chau, *Hong Kong Geological Survey Sheet 4, Solid and Superficial Geology, 1:20,000 Series HGM20*, Hong Kong Government Printer.

Hidaka, H., Shimizu, H., and Adachi, M., 2002. U-Pb geochronology and REE geochemistry of zircons from Palaeoproterozoic paragneiss clasts in the Mesozoic Kamiaso conglomerate, central Japan: evidence for an Archean provenance. *Chemical Geology*, 187: 279–293.

Hsü, K.J., Li, J.L., Chen, H.H., Wang, Q.C., Sun, S., and Sengor, A.M.C., 1990. Tectonics of south China: key to understanding west Pacific geology. *Tectonophysics*, 183: 9–39.

Jackson, S.E., Pearson, N.J., Griffin, W.L., and Belousova, E.A., 2004. The application of laser ablation-inductively coupled plasma-mass spectrometry to in situ U-Pb zircon geochronology. *Chemical Geology*, 211: 47–69.

Jahn, B.M., Wu, F.Y., Lo, C.H., and Tsai, C.H., 1999. Crust-mantle interaction induced by deep subduction of the continental crust: geochemical and Sr-Nd isotopic evidence from post-collisional mafic-ultramafic intrusions of the northern Dabie complex, central China. *Chemical Geology*, 157 (1–2): 119–146.

Jiang Yang, Yeung Kaming, Yang Zhuliang, Shen Jialin, Ma Xue, Chan Yunam, Qian Maiping, Xing Gugangfu, Yu Minggang and Duan Zheng, 2016. Stratigraphic study on Upper Jurassic Laichichong (Lai Chi Chong) Formation in the Hong Kong Global Geopark, China: rock association and diagenetic process. *Geological Review*, 62(3): 759–769 (in Chinese with English abstract).

Jones, N.S., 1995. *The sedimentology of the (Devonian) Bluff Head Formation, New Territories, Hong Kong, with sedimentological notes on other strata examined within the area*. British Geological Survey Technical Report WH/95/101R, British Geological Survey, U. K.

Jones, N.S., 1996. *The geology and sedimentology of Upper Palaeozoic and Mesozoic sedimentary successions in Hong Kong*. British Geological Survey Technical Report WH/96/130R, British Geological Survey, U. K.

Lai, K.W., 1991. Stratigraphy of the Ping Chau Formation, Hong Kong. *Geological Society Hong Kong Newsletter*, 9(2): 3–23.

Lai, K.W., Campbell, S.D.G., and Shaw, R., 1996. *Geology of the Northeastern New Territories*. Hong Kong Geological Survey Memoir No. 5, Geotechnical Control Office, Hong Kong, 144.

Lee, C.M., 1985. Recent development in Hong Kong stratigraphy. *Geological Society Hong Kong Newsletter*, 3(4): 7–9.

Liu Lei, Xu Xisheng, Xia Yan, Liang Qiongdan and Pei Xiaoli, 2017. Disintegration of Late Mesozoic Zhucun Formation in southeastern Zhejiang: Geochronology and petrogenesis of the related volcanic rocks. *Acta Petrologica Sinica*, 33(1): 115–126 (in Chinese with English abstract).

Li Xiaochi, 2012. Regional stratigraphic division in Hong Kong. *Resources Survey & Environment*, 33(4): 211–217 (in Chinese with English abstract).

Li Zhaonai, Quan Heng, Li Zhitong, Mao Jianren, Li Hansheng, Wu Cailai, Hao Yanli, Zhang Zhaochong, Wang Bixiang and Liu Yan, 2003. *Meso-Cenozoic igneous rocks and deep processes in eastern China*. Beijing: Geological Publishing House, 257 (in Chinese).

Li Zuoming and Lin Jifeng, 1987. A discussion on features of geological structure in Hong Kong area. *Journal of Guizhou Institute of Technology*, 4: 52–66 (in Chinese with English abstract).

Li Zuoming, Chen Jinhua, He Guoxiong and Li Quanwei, 1997. Stratigraphical sequence of Hong Kong. *Journal of Stratigraphy*, 21(3): 161–182 (in Chinese with English abstract).

Li, Y.H.M., Zhou, M., Lai, K.W., Chan, L.S., and Chen, W.T., 2014. Geochemical and geochronological constraints on Late Jurassic volcanic rocks at Tuen Mun, Hong Kong, with implications for the Palaeo-Pacific subduction. *International Geology Review*, 56 (4): 408–429.

Li, Z., Qiu, J.S., and Xu, X.S., 2012. Geochronological geochemical and Sr-Nd-Hf isotopic constraints on petrogenesis of late Mesozoic gabbro-granite complexes on the southeast coast of Fujian south China: insights into a depleted mantle source region and crust-mantle interactions. *Geological Magazine*, 149 (3): 459–482.

Lin Wenjing, Gan Haonan, Wang Guiling and Ma Feng, 2016. Occurrence prospect of HDR and target site selection study in Southeastern of China, *Acta Geologica Sinica*, 90(8): 2043–2058 (in Chinese with English abstract).

Liu, Y.Q., Ji, Q., Jiang, X.J., Kuang, H.W., Ji, S.A., Gao, L.F., Zhang, Z.G., Peng, N., Yuan, C.X., Wang, X.R., and Xu, H., 2013. U-Pb Zircon ages of early Cretaceous volcanic rocks in the Tethyan Himalaya at Yangzuoyong Co Lake, Nagarze, southern Tibet, and implications for the Jurassic/Cretaceous boundary. *Cretaceous Research*, 40: 90–101.

Liu, Y.S., Hu, Z.C., Gao, S., Gunther, D., Xu, J., Gao, C.G., and Chen, H.H., 2008. In situ analysis of major and trace elements of anhydrous minerals by LA-ICP-MS without applying an internal standard. *Chemical Geology*, 257 (1–2): 34–43.

Ludwig, K.R., 2003. Isoplot 3.00: A Geochronological Toolkit for Berkeley Geochronology Center, Berkeley, p. 70.

Mei Cun, Tang Yuelin, Zhang Song, Kang Zhenjiang, Guan Fuzhen, Gong Shuyun and Li Gan, 2011. Discussion on age of the Mesozoic volcanic strata from Dapeng Peninsula National Geopark in Shenzhen. *Journal of Stratigraphy*, 35(4): 454–462 (in Chinese with English abstract).

Owen, R.B., 2000. Late Cretaceous-Early Tertiary continental lacustrine basins of Hong Kong and southeast China. In: Gierlowski-Kordesch, E.H. & Kelts, K.R. (Eds.), Lake Basins through Space and Time. *AAPG Studies in Geology*, 46: 329–334.

Ruxton, B.P., 1960. The geology of Hong Kong. *Quarterly Journal of the Geological Society of Longdon*, 115: 233–260.

Sewell, R.J., and Campbell, S.D.G., 1997. Geochemistry of coeval Mesozoic plutonic and volcanic suites in Hong Kong. *Journal of the Geological Society*, 154: 1053–1066.

Sewell, R.J., Campbell, S.D.G., Fletcher, G.J.N., Lai, K.W., and Kirk, P.A., 2000. *The Pre-Quaternary Geology of Hong Kong*. Geotechnical Engineering Office, Civil Engineering Department, the Government of the Hong Kong Special Administrative Region, 181.

Sewell, R.J., Davis, D.W., and Campbell, S.D.G., 2012a. High precision U-Pb zircon ages for Mesozoic igneous rocks from Hong Kong. *Journal of Asian Earth Science*, 43: 164–175.

Sewell, R.J., Tang, D.L.K., and Campbell, S.D.G., 2012b. Volcanic-plutonic connections in a tilted nested caldera complex in Hong Kong. *Geochemistry, Geophysics, Geosystems*, 13: Q01006–Q01022.

Shen, C.B., Mei, L.F., Peng, L., Chen, Y.Z., Yang, Z., and Hong, G.F., 2012. LA-ICPMS U-Pb zircon age constraints on the provenance of Cretaceous sediments in the Yichang area of the Jianghan Basin, central China. *Cretaceous Research*, 34: 172–183.

Tang, D.L.K., Seward, D., Wilson, C.J.N., Sewell, R.J., Carter, A., and Paul, B.T., 2014. Thermotectonic history of SE China since the Late Mesozoic: insights from detailed thermochronological studies of Hong Kong. *Journal of the Geological Society*, 171(4): 591–604.

Wang Dezi and Du Yangsong, 1990. Tectonic setting of Late Mesozoic granitic volcanic-intrusive complexes in Southeastern China. *Bulletin of Mineralogy Petrology and Geochemistry*, 3: 186–188 (in Chinese).

Wang Dezi, Zhou Jincheng, Qiu Jiansheng and Fan Honghai, 2000. Characteristics and petrogenesis of Late Mesozoic granitic volcanic-intrusive complexes in Southeastern China. *Geological Journal of China Universities*, 6(4): 487–498 (in Chinese with English abstract).

Wang Jinrong, Hu Yongbin, Chen Bin, Huang Shufeng, Ye Yuansheng, Luo Xiaohua and Lv Xinbiao, 2017. Geochemistry, geochronology and mineralization of the rare-metal granites in the Daping Ta-Nb deposit, Fujian Province, South China. *Acta Geologica Sinica* (English Edition), 91 (supp. 1): 289–290.

Wang Liming, Wang Jun, Wang He, Bu An, Guo Rui, Wang Yongquan and Zhu Peiyun, 2016. New Understanding of Dynamometamorphism Mineralization of the Faulting Zone in Lianhua- shan of Guangdong Province. *Geological Review*, 62 (S1): 90–92 (in Chinese with English abstract).

Wang, L.L., Tian, M.Z., and Wang, L., 2015. Geodiversity, geoconservation and geotourism in Hong Kong Global Geopark of China. *Proceedings of the Geologists' Association*, 126: 426–437.

Wang Lulin, Zhao Longlong, Tian Mingzhong, Wu Fadong and Zhang Xujiao, 2018. Late Jurassic to Early Cretaceous volcanism of Hong Kong: Insights from the Ping Chau Formation. *Geoscience Frontiers*, 702.

Wang, W., Liu, S.W., Feng, Y.G., Li, Q.G., Wu, F.H., Wang, Z.Q., Wang, R.T., and Yang, P.T., 2012b. Chronology, petrogenesis and tectonic setting of the Neoproterozoic Tongchang dioritic pluton at the northwestern margin of the Yangtze Block: constraints from geochemistry and zircon U-Pb-Hf isotopic systematics. *Gondwana Research*, 22 (2): 699–716.

Wang, W., Liu, S.W., Wilde, S.A., Li, Q.G., Zhang, J., Bai, X., Yang, P.T., and Guo, R.R., 2012a. Petrogenesis and geochronology of Precambrian granitoid gneisses in western Liaoning province: constraints on Neoarchean to early Paleoproterozoic crustal evolution of the north China Craton. *Precambrian Research*, s222–223(3): 290–311.

Wiedenbeck, M., Alle, P., Corfu, F., Griffin, W.L., Meier, M., Oberli, F., Vonquadt, A., Roddick, J.C., and Speigel, W. 1995. Three natural zircon standards for U-Th-Pb, Lu-Hf, trace element and REE analysis. *Geostandards Newsletter*, 19(1): 1–23.

Wiedenbeck, M., Hanchar, J.M., Peck, W.H., Sylvester, P., Valley, J., Whitehouse, M., Kronz, A., Morishita, Y., and Nasdala, L., 2004. Further characterisation of the 91500 zircon crystal. *Geostandards and Geoanalytical Research*, 28 (1): 9–39.

Williams, M.Y., 1943. The stratigraphy and palaeontology of Hong Kong and the New Territories. *Transactions of the Royal Society of Canada*, 37: 93–117.

Wu Yuanbao and Zheng Yongfei, 2004. Study on the genesis of zircon and its restrictions on explaining the U-Pb age. *Chinese Science Bulletin*, 49: 1589–1604 (in Chinese with English abstract).

Xie Qifeng, Cai Yuanfeng, Dong Yunpeng, Li Dunpeng and Lin Rongfeng, 2017. LA-ICP-MS zircon U-Pb geochronology and Hf isotopic compositions of Yanshanian granites in the Shanghang area, Fujian Province. *Acta Geologica Sinica*, 91 (10): 2212–2230 (in Chinese with English abstract).

Yao Jianxin, Bao Jingbang, Hou Hongfei, Wang Zejiu, Ma Xiulan, Liu Fengshan, Hu Guangxiao, Ji Zhangsheng, Wu Guichun, Wu Zhenjie, Li Suping, Guo Caiqing and Li Ya, 2016. Status of stratigraphy research in China. *Acta Geologica Sinica* (English Edition), 90(4): 1069–1081.

Yuan Qian, Cao Xiaofeng, Lü Xinbiao, Wang Xxiangdong, Yang Enlin, Liu Yuegao, Ruan Banxiao, Liu Hong and Munir Mohammed Abdalla Adama, 2014. LA-ICP-MS U-Pb zircon geochronology and Hf isotope, geochemistry and kinetics of the Daxigou anorthosite from Kuruqtagh block, NW China. *Chinese Journal of Geochemistry*, 33 (3): 207–220.

Zhang Jiefang, 1987. Red beds age and their classification and correlation in Hong Kong. *The journal of geological society of Guangdong province*, 1: 67–72 (in Chinese with English abstract).

Zhao Longlong, 2017. *Study on stratigraphic chronology and sedimentary environment of Port Island, Hong Kong*. Beijing: China University of Geosciences (Ph. D thesis): 1–152 (in Chinese with English abstract).

Zhao Longlong, Wang Lulin, Tian Mingzhong and Wu Fadong, 2017. Geochemistry and zircon U-Pb geochronology of the rhyolitic tuff on Port Island, Hong Kong: Implications for early Cretaceous tectonic setting. *Geoscience Frontiers*, 8(3): 565–581.

Zhou Jian, Xu Shanfa, Chi Q inghua, Chen Enke Zhang Bimin and Wang Wei, 2012. Geochemical characteristics of the Mesozoic volcanic belt in southeast coast of China. *Earth Science Frontiers*, 19 (3): 93–100 (in Chinese with English abstract).

Zhou Liyun, Wang Yu, Hei Huixin and Zhou Xiaohui, 2016. Early Cretaceous magma mingling in Xiaocuo, southeastern China continental margin: Implications for subduction of paleo-pacific plate. *Acta Geologica Sinica* (English Edition), 90(5): 1713–1742.

About the first author

ZHAO Longlong, female; born in 1988 in Shandong Province; Post-doctoral fellow of Institute of Remote Sensing and Digital Earth, Chinese Academy of Sciences. She is a PhD graduate of China University of Geosciences (Beijing). Her major is Quaternary geology and study orientation is the evaluation and planning of geological landscape.